



Sudan University of Science and Technology
Collage of Graduate Studies



**Preparation of High-Temperature Superconductor
Component $Ba_2PbCa_2Cu_3O_9$**

**تحضير المركب $Ba_2PbCa_2Cu_3O_9$ ذو التوصيلية الفائقة عند درجة
الحرارة العالية**

*A thesis submitted for partial fulfillments of the
requirement of the degree of science master in physics*

By:

Mohamed Merghni Osman Ahmed

Supervision:

Dr. Rawia Abd Elgani Elobaid Mohammed

February 2017

الآية

بسم الله الرحمن الرحيم

(فَمَنْ يُرِدِ اللَّهُ أَنْ يَهْدِيَهُ يَشْرَحْ صَدْرَهُ لِلْإِسْلَامِ وَمَنْ يُرِدْ أَنْ يُضِلَّهُ يَجْعَلْ
صَدْرَهُ ضَيِّقًا حَرَجًا كَأَمَّا يَصْعَدُ فِي السَّمَاءِ كَذَلِكَ يَجْعَلُ اللَّهُ الرِّجْسَ
عَلَى الَّذِينَ لَا يُؤْمِنُونَ)

صدق الله العظيم

(سورة الأنعام الآية 125)

Dedication

I dedicate to all those who contributed in education

Dedicate to my mother & my father

To my brothers and sister &

My teacher &

My colleagues

To all of you dedicate this modest effort

Researcher

Acknowledgements

Thank God first and foremost

Thank everyone who helped me in my career complete educational and completion of this research, and I especially thank my mother and

My father

I thank the professors Sudan University of Science and Technology Faculty of Science, Department of Physics

And thanks to my supervisor, Dr.Rawia Abdelgani

Also, I would like to thank Mr. Ali Suleiman

And Mr. Mohammed Mansour, Sudan University of Science and Technology Faculty of Science, Department of Physics

And thanks, Mr. Osman Ali, Omdurman Islamic University Faculty of Science and Technology, Department of Chemistry

God bless all of us

Abstract

The superconducting phenomenon in general was studied, and the sample of $\text{Ba}_2\text{PbCa}_2\text{Cu}_3\text{O}_9$ superconductor was prepared by solid state reaction method. Also the critical temperature of the $\text{Ba}_2\text{PbCa}_2\text{Cu}_3\text{O}_9$ superconductor was observed near 298K.

المستخلص

درست ظاهرة التوصيل الفائق بصورة عامة، كما حضرت عينة من المركب $Ba_2PbCa_2Cu_3O_9$ فائق التوصيل باستخدام طريقة تفاعل الحالة الصلبة، وعند درجة حرارة مرتفعة قريبة من 298 كلفن لوحظت ظاهرة التوصيل الفائق للمركب $Ba_2PbCa_2Cu_3O_9$.

Contents

| Title | Page |
|--|-------------|
| الأية | I |
| Dedication | II |
| Acknowledgements | III |
| Abstract | IV |
| المستخلص | V |
| Contents | VI |
| Table of Figures | IX |
| Chapter One | |
| Introduction | |
| 1.1 Superconductivity | 1 |
| 1.2 Research Problem | 1 |
| 1.3 Aims | 1 |
| 1.4 Research Significance | 2 |
| 1.5 Literature Review | 2 |
| 1.6 Research Layout | 3 |
| Chapter Two | |
| The Theoretical Background | |
| 2.1 Introduction | 4 |
| 2.2 Meissner - Ochsensfeld Effect | 5 |
| 2.3 Type I And Type II Superconductors | 6 |
| 2.4 The London Equation | 8 |
| 2.5 Bardeen-Cooper-Schrieffer (BCS) Theory | 11 |
| 2.5.1 Some BCS Theory Results | 11 |
| 2.6 Characteristics of The Superconducting State | 12 |

| | |
|---|----|
| 2.6.1 The Resistance | 12 |
| 2.6.2 The Specific Heat | 13 |
| 2.6.3 Isotope Effect | 13 |
| 2.6.4 The Coherence Length | 14 |
| 2.6.5 Ultrasonic Attenuation | 14 |
| 2.7 Flux Quantization | 14 |
| 2.8 Josephson Effect | 16 |
| Chapter Three | |
| High Temperature Superconductors | |
| 3.1 Introduction | 17 |
| 3.2 The Carrier-Phonon Coupling | 19 |
| 3.3 Layered Materials And Their Electronic Structure | 20 |
| 3.4 Crystal Structure of High Temperature Superconductors. | 20 |
| 3.4.1 $\text{La}_{2-x}\text{Ba}_x\text{CuO}_4$ | 20 |
| 3.4.2 $\text{La}_{2-x}\text{Sr}_x\text{CuO}_4$ | 22 |
| 3.4.3 $\text{YBa}_2\text{Cu}_3\text{O}_7$ | 23 |
| 3.4.4 Thallium and Mercury Based Compounds | 24 |
| 3.5 Doping of High Temperature Superconducting Materials | 25 |
| 3.6 Energy Gap Properties of Superconductors | 25 |
| 3.7 Effect of High Pressure on Superconductivity | 26 |
| 3.8 Superconductivity without Cooling | 27 |
| 3.9 Superconductivity At Room-Temperature | 27 |
| 3.10 Superconductivity Above 100 Celsius | 28 |
| 3.11 Preparation of High- T_C Superconductors | 28 |
| 3.12 Measuring The Electrical Resistance of High- T_C Superconductors | 28 |
| 3.12.1 Four-Point Probe Method | 28 |
| 3.13 Applications of Superconductors | 29 |

| | |
|---|----|
| Chapter Four | |
| Practical | |
| 4.1 Introduction | 31 |
| 4.2 Equipment Used in Preparation of The Sample | 31 |
| 4.3 The Sample Preparation | 31 |
| 4.4 Description Sample Preparation | 32 |
| 4.5 Measuring The Electrical Resistance | 33 |
| 4.5.1 Used Equipment | 33 |
| 4.5.2 Method Description of Measuring The Electrical Resistance | 33 |
| 4.6 Results | 35 |
| 4.7 Discussion | 37 |
| 4.8 Conclusion | 37 |
| 4.9 Recommendation | 37 |
| References | 38 |

Table of Figures

| Title | Page |
|--|------|
| Figure (2.1) Resistance as a function of temperature for a mercury sample | 5 |
| Figure (2.2) The Meissner effect in a superconductor | 6 |
| Figure (2.3) Illustration of the dependence of the magnetization on the applied magnetic field for type I and type II superconductors | 7 |
| Figure (2.4) Illustration of the above example of a semi-infinite superconductor in a homogeneous magnetic field in vacuum | 10 |
| Figure (2.5) Schematic illustration of the flux penetration in the Shubnikov phase | 16 |
| Figure (3.1) Timeline of superconductors and their transition temperatures | 19 |
| Figure (3.2) Crystal structures of (a) $\text{La}_{2-x}\text{Ba}_x\text{CuO}_4$ and (b) $\text{Nd}_{2-x}\text{Ce}_x\text{CuO}_4$ superconductors | 21 |
| Figure (3.3) Crystal structure of $\text{La}_{2-x}\text{Sr}_x\text{CuO}_4$ | 22 |
| Figure (3.4) Crystal structure of $\text{YBa}_2\text{Cu}_3\text{O}_{7-x}$ superconductor showing two adjoining pyramid - type CuO_2 planes and CuO chains in the unit cell | 23 |
| Figure (4.1) Sensitive balance | 31 |
| Figure (4.2) Furnace | 31 |
| Figure (4.3) Gate mortar | 32 |
| Figure (4.4) Ceramic boat | 32 |
| Figure (4.5) Circuit diagram | 34 |

Chapter One

Introduction

1.1 Superconductivity

Superconductivity is a phenomenon exhibited by certain materials by virtue of which they lose all their electric resistance below certain sufficiently low temperature accompanied by a total expulsion of magnetic field from within. These two properties (zero resistance and perfect diamagnetism) straight away imply revolutionary applications of these materials ranging from loss-less transmission lines, more efficient energy production, computers with reduced size and power consumption, very strong magnets, levitating trains to medical diagnostics etc. However, for a very long time after the discovery, the practical applications could not be realized mainly because superconductivity appeared to be a very low temperature phenomenon and the materials had to be cooled to below liquid helium temperatures which are expensive as well as difficult to handle [1].

1.2 Research Problem

The problem for this research is the superconductors become available in room temperature.

1.3 Aims

- Studying the superconductivity phenomenon.
- Preparation and determining the critical temperature of $\text{BaPbCa}_2\text{Cu}_3\text{O}_9$ high temperature superconducting.

1.4 Research Significance

High temperature superconductors is now very well understood, it is a very active field of with many practical and theoretical aspect.

1.5 Literature Review

The idea that the electrical resistance of a material would go to zero as temperature decreased was first proposed by James Dewar and John Ambrose Fleming, who conjectured that metals would become perfect electrical conductors at absolute zero. The first experimental discovery happened in 1911 when Kammerlingh Onnes found that mercury had zero resistance below 4.2 K, using liquid helium as a coolant. Soon after several other materials were found to superconductor, but none at temperatures above approximately 15 K, while theoretical work on superconductors continued the next experimental breakthrough in superconductivity came in 1986 when Bednorz and Mueller found a lanthanum based ceramic that superconductor at temperatures just below 35 K, a temperature believed before to be forbidden for superconductor. This was quickly followed with Paul Chu and M. K. Wu's replacement of the lanthanum with yttrium, which creates a superconductor called YBCO with a critical temperature of around 93 K [2].

This was economically important because this is above the boiling point of liquid nitrogen, 77 K, meaning the cheap and easily available nitrogen could be used as coolant for a superconductor instead of the more expensive helium [3].

1.6 Research Layout

This research has come into Four chapters, chapter one is introduction ,chapter two theoretical background, chapter three the high temperature superconductors, while chapter four the practical.

Chapter Two

The Theoretical Background

2.1 Introduction

The superconducting state is a phase of matter, it is observed in a wide class of materials, and however, the theoretical description includes numerous subtleties. Today the phenomenon is (basically) well understood but the development of appropriate theoretical models and the corresponding experimental inspections display many aspects of the development of physics in the 20th century.

In 1911 Kamerlingh Onnes, three years after he first liquefied helium, observed that the electrical resistance of mercury drops to an immeasurable low value below the critical temperature of $T_C \approx 4.2$ K. In fact it is fundamentally impossible to show that the resistance is exactly zero, but it is possible to give an upper limit. K. Onnes classified the first superconducting state with an upper limit to the resistance of $10^{-5}\Omega$. However, the more surprising fact was that the resistance did not increase with an increase of impurities in the mercury sample. Moreover, the resistance drops discontinuously within a temperature range of less than 0.01 K [1].

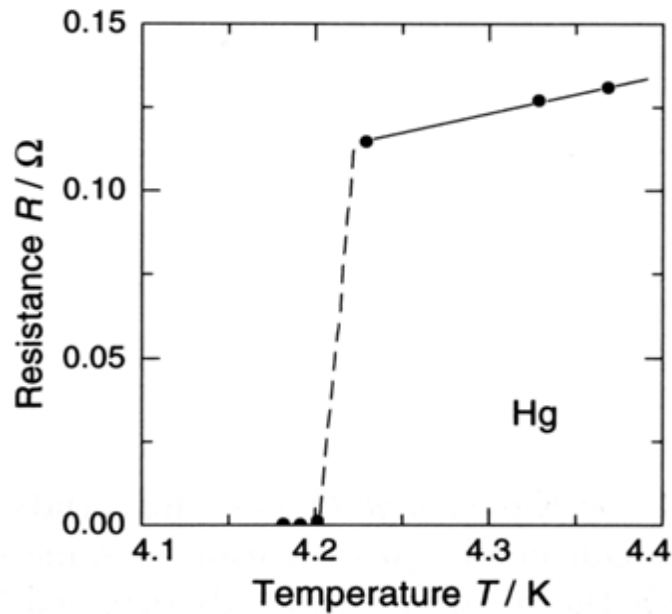


Figure (2.1) Resistance as a function of temperature for a mercury sample as investigated

2.2 Meissner - Ochsenfeld Effect

In 1933 Meissner and Ochsenfeld observed that if a superconductor within an external magnetic field B is cooled below the transition temperature T_C , then the magnetic field is pushed out of the interior of the superconductor, i.e. $B = 0$ within the superconductor. This observation has several consequences. For instance, in case of a superconducting wire we can immediately deduce that current cannot flow within the superconductor due to Ampere's law $\nabla \times B = \mu_0 J$, with μ_0 the permeability of free space and J the current density. The current must therefore flow in the surface of the wire. A second consequence is that a superconductor is not equal to an ideal conductor. For an ideal conductor we obtain from Ohm's law $E = \rho J$, with E the electrical field and ρ the resistivity, that $E \rightarrow 0$ in the limit $\rho \rightarrow 0$, since $J < \infty$ within the superconductor. However, from Maxwell's equations we now deduce that $\dot{B} \sim \nabla \times E = 0$. This is not equivalent to the observation by Meissner and Ochsenfeld since in the case of an

ideal conductor we obtain that the magnetic field must not change on cooling through the transition temperature. Hence, we obtain that perfect diamagnetism is an essential property of the superconducting state [1].

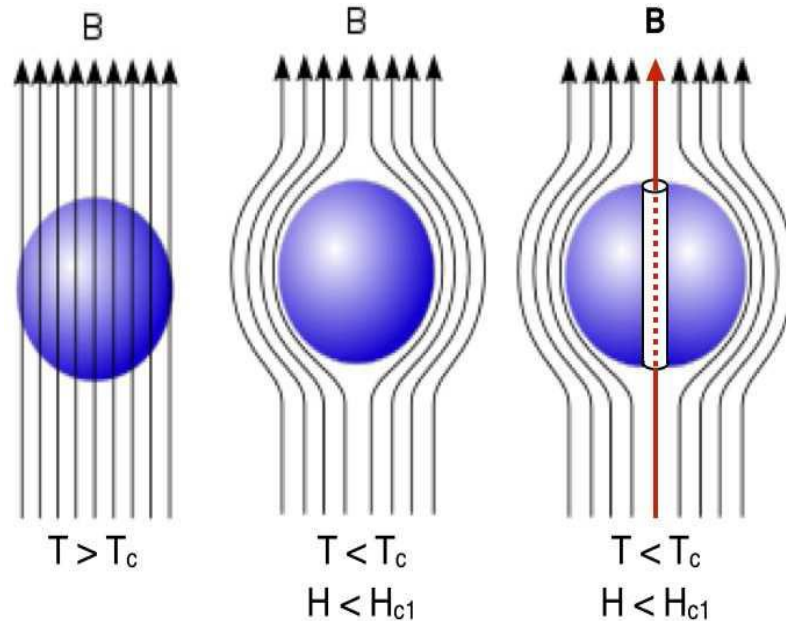


Figure (2.2) The Meissner effect in a superconductor.

2.3 Type I And Type II Superconductors

In case of type I superconductors (complete Meissner -Ochsenfeld effect) the magnetization above the critical field. Type I superconductors are typically pure materials with low values of electrical resistance.

In a type II superconductor there are two different critical fields, denoted H_{C1} , the lower critical field, and H_{C2} the upper critical field. For small values of applied field H the Meissner-Ochsenfeld effect again leads to $M = -H$ and there is no magnetic flux density inside the sample, $B = 0$. However in a type II superconductor once the field exceeds H_{C1} , magnetic flux does start to enter the superconductor and hence $B \neq 0$, and M is closer to zero than the full Meissner-Ochsenfeld value of $-H$. Upon increasing the field H further the magnetic flux density gradually increases, until finally at H_{C2} the superconductivity is

destroyed and $M = 0$. This behaviour is sketched on the right hand side of figure (2.3) [3].

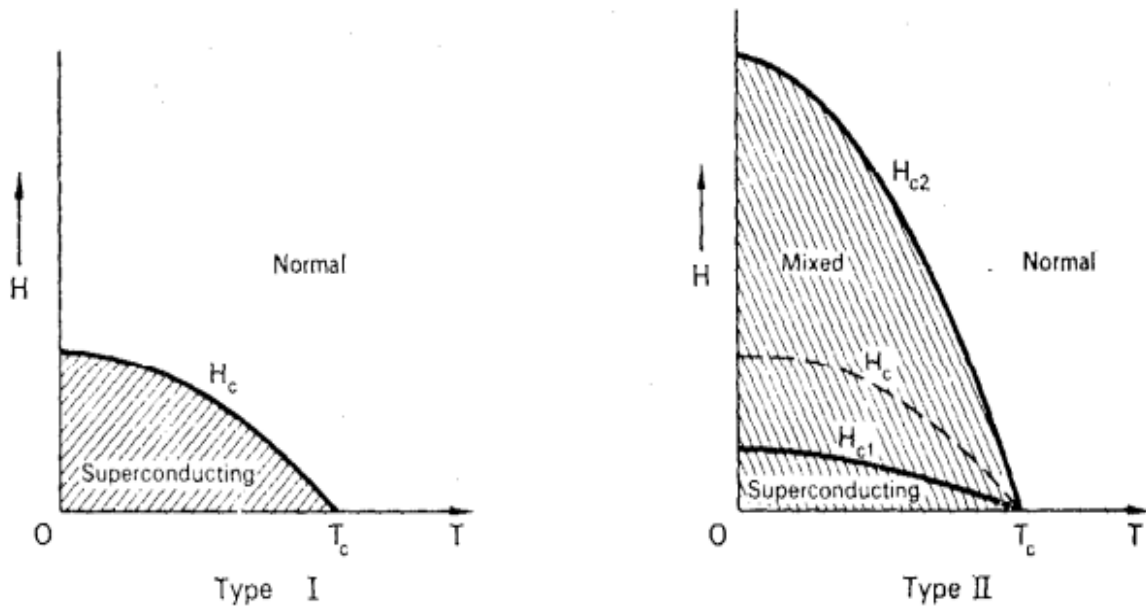


Figure (2.3) Illustration of the dependence of the magnetization on the applied magnetic field for type I and type II superconductors

The left figure shows the phase diagram of a type I superconductor. Every state that is above this line is in its normal, non-superconductive, state. However, every state below the line is in its superconductive state. When the temperature hits the critical temperature T_C , there is no superconductive state and the material will always be in its normal state. The right figure shows the phase diagram for a type II superconductor as a solid line. When a state is between H_{C1} and H_{C2} the material is in its intermediate or mixed state, where the magnetic field is able to penetrate the material and form vortices. Below H_{C1} and above H_{C2} are the superconductive and normal states respectively. For comparison, the phase diagram of a type I superconductor is shown as a dashed line [4].

2.4 The London Equation

It is the aim of the following considerations to derive the Meissner - Ochsenfeld effect from a particular ersatz for the electrodynamics laws in the superconducting state. We write the equation of motion of a charged particle in an electrical field E

$$m \dot{v} = -q E \quad (2.1)$$

Where

$m \equiv$ mass of electron.

$v \equiv$ velocity of electron.

$q \equiv$ charge of electron.

We now insert the current density

$$J_S = -q n_s v \quad (2.2)$$

n_s is the density of superconducting electrons, in order to obtain the first London equation

$$\frac{\partial J_S}{\partial t} = \frac{n_s q^2}{m} E \quad (2.3)$$

From $\nabla \times E = -\frac{\partial B}{\partial t}$ we obtain

$$\frac{\partial}{\partial t} \left(\frac{m}{n_s q^2} \nabla \times J_S + B \right) = 0 \quad (2.4)$$

This equation describes an ideal conductor, i.e. $\rho = 0$. However, the expulsion of the magnetic field in the Meissner - Ochsenfeld effect is not yet included. Integrating this equation with respect to time and neglecting the integration

constant yields the second London equation, which already includes correcting physical description:

$$\nabla \times \mathbf{J}_S = -\frac{n_s q^2}{m} \mathbf{B} \quad (2.5)$$

From $\mathbf{B} = \nabla \times \mathbf{A}$, where \mathbf{A} is the vector potential, can conclude that

$$\mathbf{J}_S = -\frac{n_s q^2}{m} \mathbf{A} \equiv -\frac{1}{\mu_0 \lambda_L^2} \mathbf{A} \quad (2.6)$$

Where we defined $\lambda_L = \sqrt{\frac{m}{n_s \mu_0 q^2}}$ with the dimension of length (often noted as λ_L is called the London penetration depth), and μ_0 is the permeability of free space. Here, \mathbf{A} has to be understood in the London gauge. For a simply connected superconductor it may be expressed by $\nabla \cdot \mathbf{A} = 0$.

The second London equation can be rewritten in the following way

$$\nabla \times \mathbf{J}_S = -\frac{1}{\mu_0 \lambda_L^2} \mathbf{B} \quad (2.7)$$

Further, from Maxwell's equations

$$\nabla \times \mathbf{B} = \mu_0 \mathbf{J}_S \quad (2.8)$$

We obtain

$$\nabla \times \nabla \times \mathbf{B} = -\nabla^2 \mathbf{B} = \mu_0 \nabla \times \mathbf{J}_S \quad (2.9)$$

Combining eqs (2.7) and (2.9) yields

$$\nabla \times \mathbf{J}_S - \frac{1}{\lambda_L^2} \mathbf{B} = 0 \quad (2.10)$$

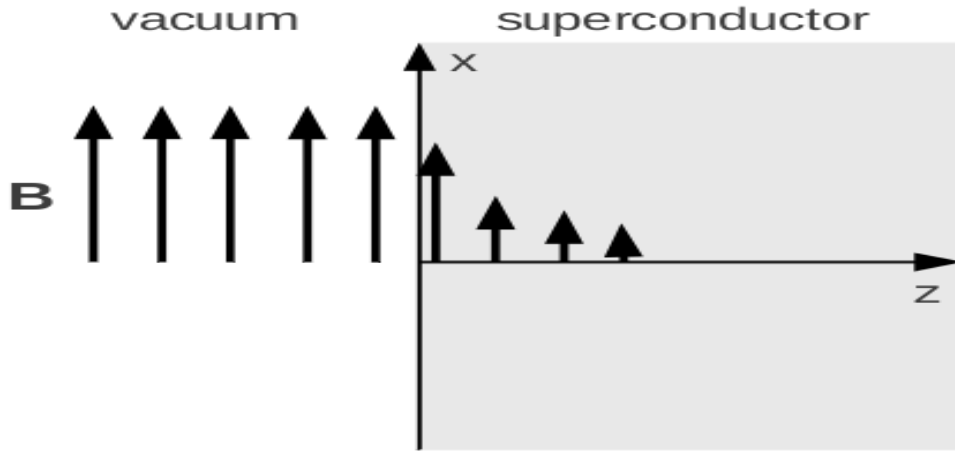


Figure (2.4) Illustration of the above example of a semi-infinite superconductor in a homogeneous magnetic field in vacuum

Equivalently, we can combine eqs (2.5) and (2.9) in order to obtain

$$\nabla^2 J_S - \frac{1}{\lambda_L^2} J_S = 0 \quad (2.11)$$

We regard a semi-infinite superconductor ($Z > 0$) in a magnetic field which is homogeneous in vacuum ($Z < 0$). In case that $\mathbf{B} = B_x \mathbf{e}_x$ we obtain from eq. (2.8) that j_S is of the form $J_S = J_{SY} \mathbf{e}_y$. We can calculate the magnetic field and the current density in the superconductor from eqs (2.10) and (2.11):

$$B_x(Z) = B_x(0) \exp\left(-\frac{Z}{\lambda_L}\right) \quad (2.12)$$

And

$$J_{SY}(Z) = J_{SY}(0) \exp\left(-\frac{Z}{\lambda_L}\right) \quad (2.13)$$

This means that the magnetic field as well as the current decay exponentially with distance into the superconductor. Here, λ_L is referred to as the London penetration depth. For a typical superconductor such as Stannum (Sn),

its value is approximately 26 nm. Hence, the London equations describe the Meissner - Ochsensfeld effect particularly well [1].

2.5 Bardeen-Cooper-Schrieffer (BCS) Theory

The BCS theory of superconductivity as developed by Bardeen, Cooper and Schrieffer in 1957, the BCS theory proved to be very important for our modern understanding of theoretical solid state physics since many concepts appearing in the framework of this theory reappeared in the context of numerous further effects and phenomena, such as the fractional quantum Hall effect, topological insulators or even in nuclear physics. The basic ingredient to a successful microscopic description is the realization that at sufficiently low temperatures two electrons form an energetically favored state through electron - phonon – electron interaction, called a Cooper pair. This attractive interaction between the electrons yields a ground state which is separated from the excited states by a band gap, as experimentally observed. Also the fact that phonons play a crucial role in the formation of this ground state was observed experimentally through the isotope effect. Most of the thermodynamic properties of superconductors are a direct consequence of the occurrence of a band gap, thus a profound understanding of Cooper pairs is essential in a microscopic description of superconductivity [1].

2.5.1 Some BCS Theory Results

- i.** Attractive interaction between electrons leads to the formation of Cooper pairs. The ground state is separated from the excited state by an energy gap. With the help of this energy gap one can explain phenomena such as the critical field, thermal properties and electromagnetic properties.
- ii.** The electron - lattice - electron interaction can be understood in an intuitive way with the help of the following simplified picture: One

electron interacts with the lattice and deforms it, the second electron is affected by the lattice deformation and moves therefore in the field of the first electron. In particular, the two electrons interact through the lattice deformation. In this attractive process the total energy is lowered.

- iii. The London equations, and therefore also the penetration depth as well as the coherence length, are a direct consequence of the BCS theory. Since the London equations account for the Meissner - Ochsensfeld effect, also this experimental fact is implicitly accounted for within the microscopic theory.
- iv. The BCS theory states that superconducting band gap $\Delta(T)$ as a function of temperature.
- v. The magnetic flux through a superconducting ring is quantized and since a Cooper pair consists of two electrons, the unit of charge is $2q$ [1].

2.6 Characteristics of the Superconducting State

2.6.1 The Resistance

The resistance goes to zero in the superconducting state. A persistent current induced magnetically to a superconducting ring has been found to decay in more than at least 10^5 years but some theoretical estimates give more than 10^{10} years.

2.6.2 The Specific Heat

The phase transition from the normal to the superconducting state is a second order phase transition in absence of a magnetic field. That means that the thermodynamic functions, as the total energy, are continuous through the transition [5].

Measurements show that for temperatures below the critical temperature,

$T < T_c$, the entropy of the system is decreased. This contains the information that the superconducting state is more ordered than the normal state. This observation was of crucial importance for the development of microscopic theories. Since the change in entropy is very small, this must mean that only a small fraction of all conduction electrons participate in the transition to the superconducting state [1].

2.6.3 Isotope Effect

It was experimentally found that different isotopes of the same superconducting metal have different critical temperatures, and

$$T_C M^\alpha = \text{constant} \quad (2.14)$$

Where M is the isotope mass, for the majority of superconducting elements,

α is close to the classical value 0.5.

The vibrational frequency of a mass M on a spring is proportional to $M^{-1/2}$, and the same relation holds for the characteristic vibrational frequencies of the atoms in a crystal lattice. Thus, the existence of the isotope effect indicated that, although superconductivity is an electronic phenomenon, it is nevertheless related in an important way to the vibrations of the crystal lattice in which the electrons move [6].

2.6.4 The Coherence Length

The coherence length is one of the important parameters describing a superconductor. It is a measure of the volume where the coherent state takes place. One can also think of it as a measure of the extension of a Cooper pair. One can intuitively think that the bigger this length, the weaker the binding between the two electrons that constitute the Cooper pair. So it is not surprising that it relates inversely to the superconducting gap and to critical temperature.

2.6.5 Ultrasonic Attenuation

In the superconducting state, the sound waves are less and less attenuated as the temperature goes to zero. This is due to the fact that the attenuation of the sound (movement of parallel planes perpendicular to the direction of the sound) creates an imbalance between the center of positive and negative charges which results in an internal electric field that accelerates the electrons. These take energy and momentum from the sound wave and eventually the sound wave is attenuated. The electrons give back the energy to the lattice but not in the coherent way to preserve the sound wave. Equilibrium is attained finally and the sample uses the sound energy to rise its temperature. In the superconducting state, the lattice does not like to take energy from the electronic system. Sound can theoretical persist into a superconductor forever at $T = 0K$ [7].

2.7 Flux Quantization

In this section we aim to reproduce the result of flux quantization in a superconducting ring. Therefore we regard a gas of charged bosons (Cooper pairs). Let ψ be the pair wave function and $n = \psi \psi^* = \text{const.}$ the total number of pairs. We express as

$$\psi = \sqrt{n} \exp(i\theta) \quad (2.15)$$

Where the phase θ may be a function of local space, the particle velocity operator is given by

$$v = \frac{1}{m} (-i\hbar\nabla - qA) \quad (2.16)$$

And, consequently, the particle flux is given by

$$\psi^* v \psi = \frac{qn}{m} (\hbar\nabla\theta - qA) \quad (2.17)$$

We can write the electric current density as

$$j = q\psi^* v \psi = \frac{qn}{m} (\hbar\nabla\theta - qA) \quad (2.18)$$

Taking the curl of both sides of this equation yields the London equation:

$$\nabla \times \mathbf{j} = \frac{q^2 n}{m} \nabla \times \mathbf{A} \quad (2.19)$$

Due to the Meissner – Ochsensfeld effect we know that $\mathbf{B} = 0$ in the interior of the superconductor. Therefore, we have $\mathbf{j} = 0$ and it follows from (2.18) that

$$q\mathbf{A} = \hbar \nabla \theta \quad (2.20)$$

We now select a closed path C through the interior of the superconductor and integrate the right hand side of (2.20)

$$\hbar \oint dL \nabla \theta = (\theta_2 - \theta_1) \quad (2.21)$$

I.e. \hbar times the change of the phase when going once around the contour C , since must not change through the integration we obtain that

$$\theta_2 - \theta_1 = 2\pi S \quad (2.22)$$

With S some integer, for the left hand side of (2.20) we obtain through Stokes' theorem

$$q \oint dL \mathbf{A} = q \int dF \cdot \nabla \times \mathbf{A} = q \int dF \cdot \mathbf{B} = q\Phi \quad (2.23)$$

The magnetic flux, Here, dF is an element of the area bounded by the contour C . Accordingly

$$\Phi = \frac{2 \hbar \pi S}{q} = \Phi_0 S \quad (2.24)$$

With the flux quantum (Φ_0), Note that in the particular case of Cooper pairs we have to replace $q \rightarrow 2q$.

In type II superconductors one observes these quantized magnetic flux tubes in the Shubnikov phase. The magnetic field penetrates the superconductor and is organized in vortices. These vortices interact with each other and are rearranged in a periodic structure (like a lattice) [1].

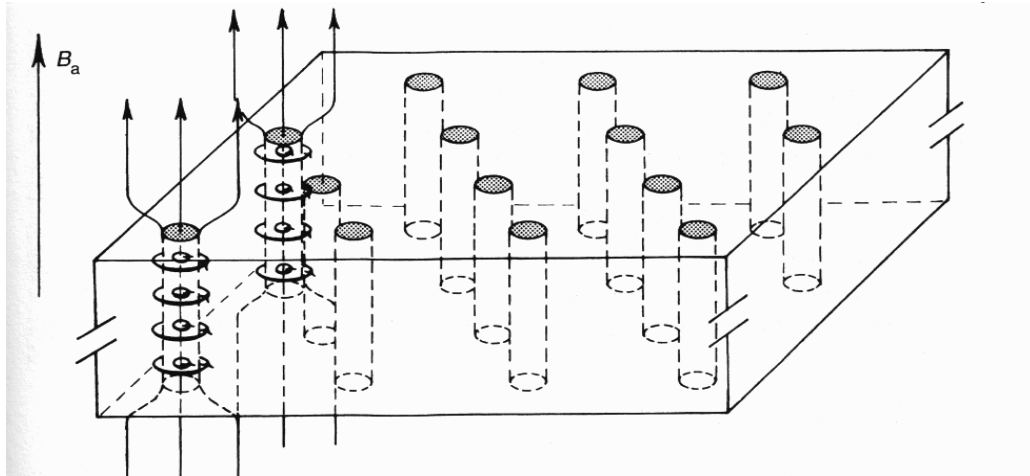


Figure (2.5) Schematic illustration of the flux penetration in the Shubnikov phase

2.8 Josephson Effect

The Josephson Effect is a direct physical test of the quantum coherence implied by superconducting. Soon after the BCS theory was published Brian Josephson, considered the effect of electrons tunneling between two different superconductors. The experimental observation of the Josephson effect not only confirmed the theory and the validity of the BCS macroscopic quantum coherent state, but also provided another direct empirical confirmation that the relevant particle charge is $(2e)$ and not (e) [5].

Chapter Three

High Temperature Superconductors

3.1 Introduction

It has long been a dream of scientists working in the field of superconductivity to find a material that becomes a superconductor at room temperature. A discovery of this type will revolutionize every aspect of modern day technology such as power transmission and storage, communication, transport and even the type of computers we make. All of these advances will be faster, cheaper and more energy efficient. This has not been achieved to date. However, in 1986 a class of materials was discovered by Bednorz and Müller that led to superconductors that we use today on a bench-top with liquid nitrogen to cool them. Not surprisingly, Bednorz and Müller received the Nobel Prize in 1987 (the fastest-ever recognition by the Nobel committee). The materials we mostly use on bench-tops is Yttrium – Barium – Copper Oxide, or $\text{YBa}_2\text{Cu}_3\text{O}_7$, otherwise known as the 1-2-3 superconductor, and are classified as high temperature (T_C) superconductors. The critical temperature of some high- T_C superconductors is given in table (3.1). Critical temperatures as high as 135 K have been achieved. Whilst this is not room temperature, it has made experiments on superconductivity accessible to more people since these need only be cooled by liquid nitrogen (with a boiling point of liquid nitrogen is 77 K), which is cheap and readily available. This is in contrast to the expensive and bulky equipment that used liquid helium for cooling the traditional types of superconductors. Moreover, the superconductors are calculated to have an upper critical magnetic field of about 200 Tesla.

Unlike traditional superconductors, conduction mostly occurs in the planes containing the copper oxide. It has been found that the critical temperature is very sensitive to the average number of oxygen atoms present, which can vary.

For this reason the formula for 1-2-3 superconductor is sometimes given as $\text{YBa}_2\text{Cu}_3\text{O}_{7-\delta}$ where δ is a number between 0 and 1.

The nominal distance between cooper pairs (coherence length) in these superconductors can be as short as one or two atomic spacings. As a result, the coulomb repulsion force will generally dominate at these distances causing electrons to be repelled rather than coupled. For this reason, it is widely accepted that Cooper pairs, in these materials, are not caused by a lattice deformation, but may be associated with the type of magnetism present (known as ant ferromagnetism) in the copper oxide layers. So high temperature superconductors cannot be explained by the BCS theory since that mainly deals with a lattice deformation mediating the coupling of electron pairs. The research continues into the actual mechanism responsible for superconductivity in these materials [5].

Table (3.1) The critical temperatures of some superconductors.

| Element | T_c (K) | Element | T_c (K) | Element | T_c (K) |
|---|-----------|--|-----------|---|-----------|
| Al | 1.19 | Nb | 9.2 | Tc | 7.8 |
| Be | 0.026 | Np | 0.075 | Th | 1.37 |
| Cd | 0.55 | Os | 0.65 | Ti | 0.39 |
| Ga | 1.09 | Pa | 1.3 | Tl | 2.39 |
| Hf | 0.13 | Pb | 7.2 | U | 0.2 |
| Hg | 4.15 | Re | 1.7 | V | 5.3 |
| In | 3.40 | Rh | 0.0003 | W | 0.012 |
| Ir | 0.14 | Ru | 0.5 | Zn | 0.9 |
| La | 4.8 | Sn | 3.75 | Zr | 0.55 |
| Mo | 0.92 | Ta | 4.39 | | |
| Compound | T_c (K) | Compound | T_c (K) | Compound | T_c (K) |
| Nb_3Sn | 18.1 | MgB_2 | 39 | UPt_3 | 0.5 |
| Nb_3Ge | 23.2 | PbMo_6S_8 | 15 | UPd_2Al_3 | 2 |
| Cs_3C_{60} | 19 | $\text{YPd}_2\text{B}_2\text{C}$ | 23 | $(\text{TMTSF})_2\text{ClO}_4$ | 1.2 |
| Cs_3C_{60} | 40 | $\text{HoNi}_2\text{B}_2\text{C}$ | 7.5 | $(\text{ET})_2\text{Cu}[\text{Ni}(\text{CN})_2]\text{Br}$ | 11.5 |
| High- T_c superconductor | T_c (K) | High- T_c superconductor | T_c (K) | | |
| $\text{La}_{1.83}\text{Sr}_{0.17}\text{CuO}_4$ | 38 | $\text{Tl}_2\text{Ba}_2\text{Ca}_2\text{Cu}_3\text{O}_{10+x}$ | 125 | | |
| $\text{YBa}_2\text{Cu}_3\text{O}_{6+x}$ | 93 | $\text{HgBa}_2\text{Ca}_2\text{Cu}_3\text{O}_{8+x}$ | 135 | | |
| $\text{Bi}_2\text{Sr}_2\text{Ca}_2\text{Cu}_3\text{O}_{10+x}$ | 107 | $\text{Hg}_{0.8}\text{Tl}_{0.2}\text{Ba}_2\text{Ca}_2\text{Cu}_3\text{O}_{8.33}$ | 134 | | |

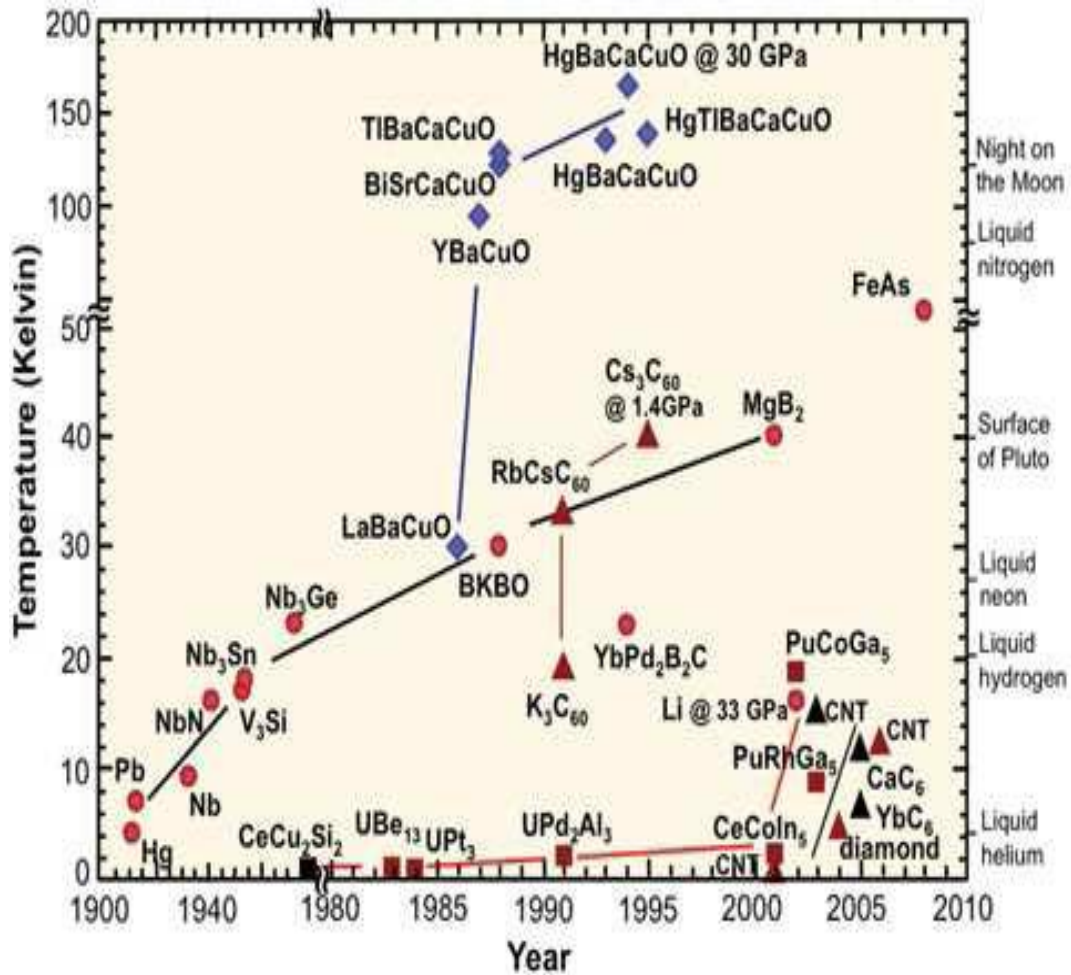


Figure (3.1) Timeline of superconductors and their transition temperatures.

3.2 The Carrier-Phonon Coupling

In conventional superconductors, a very important parameter is the coupling between the electrons and the phonons in conventional superconductivity. Cooper pairs in most of the high temperature superconductivity (HTSC) are composed by holes on the CuO_2 planes. Nobody knows whether superconductivity is phonon-mediated or not. To be able to judge on that possibility, it is important to know the value of the hole-phonon coupling parameter in these materials.

It has not been easy to measure accurately the phonon spectrum for the high temperature superconductivity (HTSC) and to identify the different modes [6].

3.3 Layered Materials and Their Electronic Structure

In general, all high temperature superconducting materials are basically tetragonal with a lattice constant of about 3.8 Å and consist of one or more CuO₂ planes in their structure, which are separated by layers of other atoms (Ba, La, O...). The in plane oxygen bond length is about 1.9 Å. As mentioned above, most researchers in this field believe that superconductivity is related to processes occurring in the CuO₂ planes, whereas the other layers simply provide the carriers. All high temperature superconductivity (also called cuprates) has such charge reservoirs.

The superconducting transition temperature T_C seems to depend on the number of CuO₂ planes per unit cell; for example, the three layer Hg and Tl compounds have a T_C of 134 K and 127 K, respectively. The fact that T_C increases with the number of layers has led to speculation about increasing T_C up to room temperature which, however, has not been realized up to now [8].

3.4 Crystal Structure of High Temperature Superconductors

3.4.1 La_{2-x}Ba_xCuO₄

La_{2-x}Ba_xCuO₄ (x is number) discovered in 1986, is a copper oxide superconductor. This material became the forerunner of the series of high T_C superconductor discoveries which followed. The basis of high critical temperature (T_C) superconductors is the CuO₂ layer. This layer becomes the platform for the superconductivity occurrence. The high T_C superconductors are also called the cuprate superconductors.

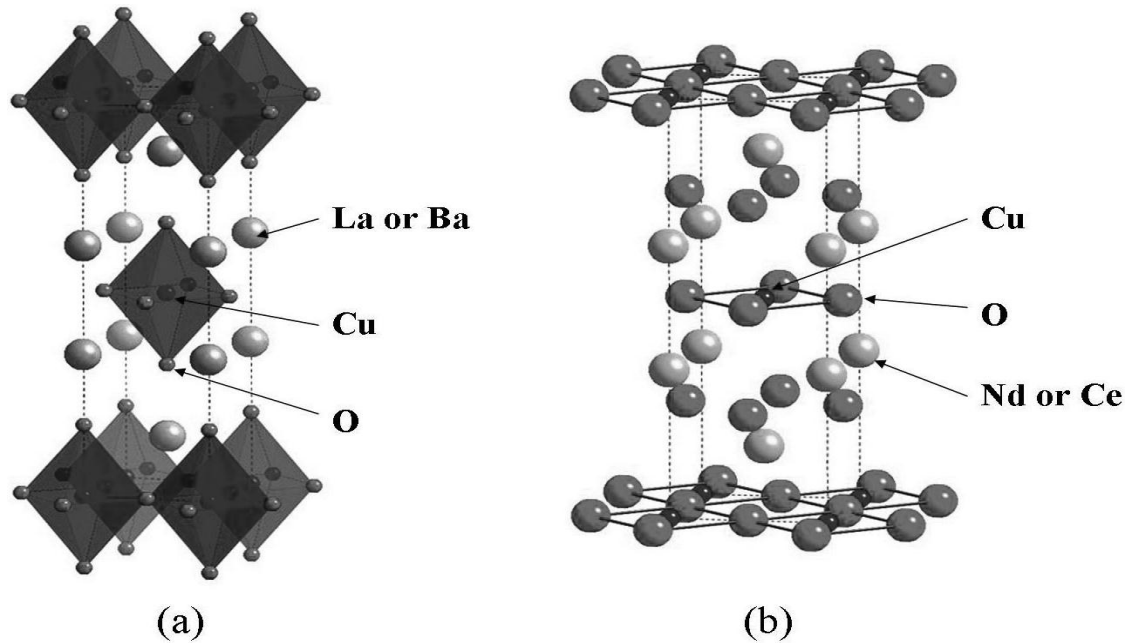


Figure (3.2) Crystal structures of (a) $\text{La}_{2-x}\text{Ba}_x\text{CuO}_4$ and (b) $\text{Nd}_{2-x}\text{Ce}_x\text{CuO}_4$ superconductors.

The crystal structures of $\text{La}_{2-x}\text{Ba}_x\text{CuO}_4$ and $\text{Nd}_{2-x}\text{Ce}_x\text{CuO}_4$ superconductors are shown in Figure (3.2) $\text{La}_{2-x}\text{Ba}_x\text{CuO}_4$, in which some of the La^{3+} ions are substituted by Ba^{2+} ions [9].

This material has a layer structure in which the (La, Ba) layers and the CuO_6 octahedrons are stacked alternately, and the CuO_2 layers are formed parallel to the bottom face. Although LaCuO_4 itself is in the antiferromagnetic state, as the concentration x of Ba^{2+} ions increases, the holes that become carriers are implanted into the CuO_2 layers, and concurrently T_C starts to increase, achieving a maximum value of 38 K.

3.4.2 $\text{La}_{2-x}\text{Sr}_x\text{CuO}_4$

This compound, usually abbreviated to LSCO, crystallizes in a body-centered tetragonal structure and is shown in figure (3.3). The CuO_2 planes are approximately (6.6\AA) are apart and separated by two LaO planes, which form the

charge reservoir. Each copper atom in the conducting planes has a bond to oxygen atoms above and below in the c direction, which are called apical oxygen. This is typical for all hole – doped high – T_C cuprate materials.

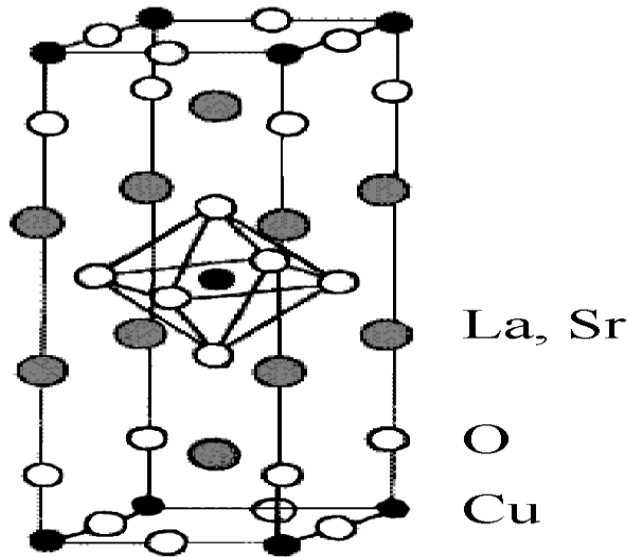


Figure (3.3) Crystal structure of $\text{La}_{2-x}\text{Sr}_x\text{CuO}_4$

Furthermore, the Cu ions are surrounded by octahedral of oxygen. The Cu–O bond in the (c) direction is much weaker than in the (a b) plane because its length is considerably larger ($\sim 2.4 \text{ \AA}$) than the Cu–O distance in the CuO_2 planes ($\sim 1.9 \text{ \AA}$). Thus the dominant bonds are those in the planes, and the importance of the apical oxygen is still under discussion [10].

3.4.3 $\text{YBa}_2\text{Cu}_3\text{O}_7$

$\text{YBa}_2\text{Cu}_3\text{O}_7$ (YBCO or Y123) is the superconductor whose critical temperature (T_C) was above the temperature of liquid nitrogen (77 K) for the first time and reached 93 K. In this material, layers of Y atoms are sandwiched between the two adjoining pyramid - type CuO_2 layers. Moreover, there is a triple periodic structure in which Y and Ba atoms are in line as Ba – Y – Ba, and there are also one - dimensional chains of Cu – O – Cu in the direction of the b - axis of the crystal.

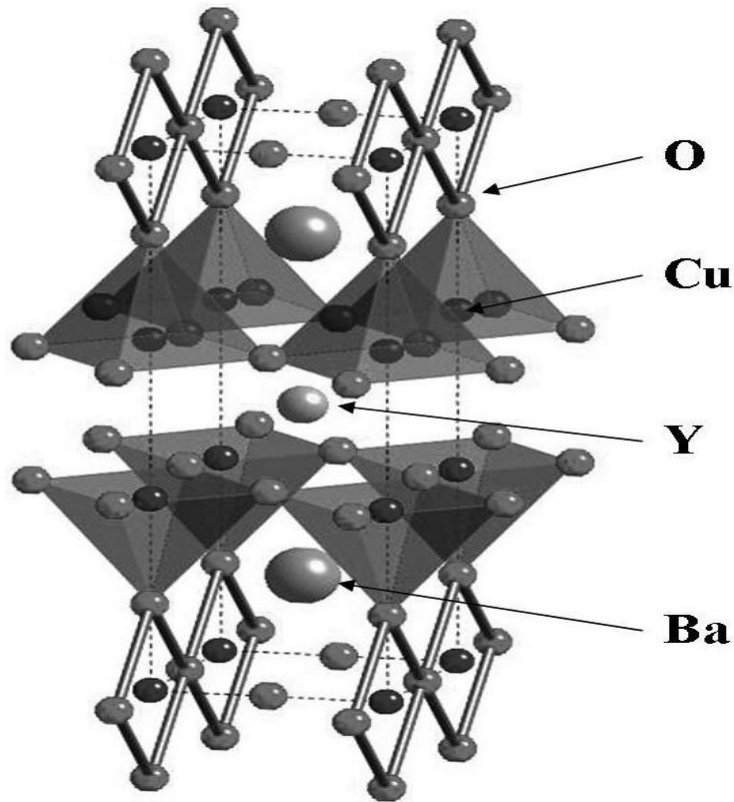


Figure (3.4) Crystal structure of $\text{YBa}_2\text{Cu}_3\text{O}_{7-x}$ superconductor showing two adjoining pyramid - type CuO_2 planes and CuO chains in the unit cell.

The oxygen deficiency, expressed by x in the chemical formulae of $\text{YBa}_2\text{Cu}_3\text{O}_{7-x}$, plays an important role in the hole implantation into CuO_2 layers. The amount of the oxygen deficiency is controlled by incomings and outgoings of the oxygen on the CuO chains [11].

3.4.4 Thallium and Mercury Based Compounds

There are several families of superconducting materials which incorporate Tl. The $\text{Tl}_2\text{Ba}_2\text{Ca}_n\text{Cu}_{n+1}\text{O}_{2n+6}$ system is analogous to the Bi based material with equivalent crystal structures and similar inter-layer spacings. In addition, the 'single Tl-O layer' $\text{TlBa}_2\text{Ca}_{n-1}\text{Cu}_n\text{O}_{2n+3}$ and $\text{TlSr}_2\text{Ca}_{n-1}\text{Cu}_n\text{O}_{2n+3}$ are superconducting.

The TSCCO compounds can be difficult to synthesise unless the Tl is partially substituted by Pb or Bi and the critical temperatures are generally lower than those of TBCCO, although they may be increased to 100 K with appropriate doping. The superconducting properties of the Tl compounds are less sensitive to oxygen stoichiometry than YBCO and in terms of anisotropy, they lie somewhere between YBCO and BSCCO. Of all the high T_C materials fabricated to date, those with the highest transition temperatures are the Hg based compounds. $\text{HgBa}_2\text{Ca}_2\text{Cu}_3\text{O}_8$, which has the same crystal structure as Tl-1223, has a T_C of 135 K, which can be increased by application of pressure. Due to the fact that the Hg compounds are closely related to the Tl materials in terms of their crystal structures, they have similar superconducting properties.

The high T_C materials have highly anisotropic crystal structures which lead to anisotropic physical properties. This anisotropy is related to the spacing between the superconducting Cu-O planes. An additional factor, which makes YBCO much less anisotropic than the other materials, is the presence of Cu-O chains between the cuprate planes [12].

3.5 Doping of High Temperature Superconducting Materials

The simplest copper oxide perovskites are insulators. In order to become superconducting, they should be doped by charge carriers. There are two ways to increase the number of charge carriers in cuprates:

- i. To substitute metallic atoms in the intermediate planes by higher-valence atoms.
- ii. To change the number of oxygen atoms. Doping increases the number electrons or holes at the Fermi level. The concentration of charge carriers in HTSC is low ($\sim 5 \times 10^{21}$), in comparison with conventional superconductors ($\sim 5 \times 10^{22} - 10^{23}$). However, due to the large coherence

length in conventional superconductors, only a 10^{-4} part of the electrons, located near the Fermi surface, participate in coupling. At the same time, in cuprates, $\sim 10\%$ of all conduction electrons (holes) form the Cooper pairs.

3.6 Energy Gap Properties of Superconductors

In conventional superconductors the temperature of superconductive transition T_C is directly defined by value of the superconductive gap, Δ , which presents itself as a binding energy of two coupled electrons in superconductive state. However, this situation is quite different in HTSC, where there is absent direct dependence between T_C and Δ . For example, variation of charge carrier concentration can lead to decreasing T_C , but increasing Δ . The value of Δ can be non zero at the $T > T_C$, at the same time in normal state of conventional superconductors always $\Delta = 0$.

The metals become superconductive, when their free electrons divide into the Cooper pairs, at the same time wave functions of all pairs have the same phase. The phase coherence is responsible, in particular for transformation of electric resistance to zero at the cooling lower than the superconductive transition temperature, T_C , and existence in superconductor of the coupled pairs leads to arising gap in spectrum of quasi particle excitations, which is registered by different spectroscopic methods.

In conventional lower temperature superconductors (LTSC) the phase coherence of pairs is stated practically simultaneously with their formation, therefore the electric resistance disappears at the $T = T_C$ simultaneously with arising the gap in spectrum. At the same time in HTSC, the gap is conserved also in absence of phase coherence that is in non-superconductive samples. Origin of this gap, called by pseudogap, up to date is subject of discussions. According to one of viewpoints, the pseudogap is caused by presence of coupled, but non-

coherent pairs (macroscopic phase coherence is fractured by thermal fluctuations), that is in fact to be portent of superconductivity. Advocates of alternative interpretation assume that the pseudogap forms due to proximity of HTSC to some non-superconductive (possibly, magnetic) state which competes with superconductive one and is to be a sign of existence another type of ordering (for example, spin or charge one). According to two scenarios, in HTSC simultaneously could exist either only one gap (superconducting or pseudogap), or the both together [13].

3.7 Effect of High Pressure on Superconductivity

In difference of majority superconductors, for which the critical temperature of superconductive transition T_C decreases with rise of pressure, in HTSC T_C increases usually. Studies of one-axis pressure witness that this increase in main degree is caused by decreasing a square, A , of CuO_2 planes

$$T_C \propto A^{-2} \quad (3.1)$$

Where A is area, but no distance between them. These results support theoretical models, which attribute superconductivity, in first order to intra-plane coupling interactions. Hence, the future experiments must state dependences on hydrostatic and one-axis pressure of the main parameters, namely: T_C , superconductive gap, pseudogap, carrier concentration and exchange interaction in all range of doping [14].

3.8 Superconductivity without Cooling

Superconductivity is remarkable phenomenon: Superconductors can transport electric current without any resistance and thus without any losses whatsoever. It is already in use in some niche areas, for example as magnets for nuclear spin tomography or particle accelerators. However, the materials must be

cooled to very low temperature for this purpose. But during the past year, an experiment has provided some surprises [15].

3.9 Superconductivity at Room-Temperature

Normally, extreme cold is required to cool even a high temperature superconductor below its critical temperature (T_C). To make this discovery, no cooling was required. For the first time a cryostat actually had to be heated to witness a superconductive phase transition.

The hallmark of superconductivity is a sudden resistance drop to zero ohms and strong diamagnetism (the Meissner effect) near same temperature. In numerous tests a small amount of the compound $(Tl_5Pb_2) Ba_2Mg_2Cu_9O_{17}$ consistently produced sharp resistive transitions near $28.5^\circ C$, and diamagnetic transitions also near $28.5^\circ C$. The transitions were unambiguous, repeatable, and at ambient pressure, marking this the first observation of true room-temperature superconductivity in a copper-oxide. Unfortunately, like the $18^\circ C$ superconductor discovered in March 2011[16].

3.10 Superconductivity above 100 Celsius

The successful synthesis of the first compound to exhibit superconductivity above the boiling point of water. $Sn_6Sb_6Ba_2MnCu_{13}O_{26}$ displays a critical transition temperature near $110^\circ C$ (230F, 383K). This brings to 21 the number of compounds found to display superconductivity above room temperature [17].

3.11 Preparation of High- T_C superconductors

The simplest method for preparation high- T_C superconductors is a solid-state thermochemical reaction involving mixing, calcination and sintering. The appropriate amounts of precursor powders, usually oxides and carbonates, are

mixed thoroughly using a ball mill or gate mortar. Solution chemistry processes such as precipitation, freeze-drying and sol-gel method are alternative ways for preparing a homogeneous mixture. These powders are calcined in the temperature range from 800 °C to 950 °C for several hours. The powders are cooled, reground and calcined again. The process is repeated several times to get homogeneous material [18].

3.12 Measuring the Electrical Resistance

3.12.1 Four-Point Method

The most common method of determining the T_C of a superconductor. Wires are attached to a material at four points with a conductive adhesive. Through two of these points a voltage is applied, and if the material is conductive, a current will flow. Then, if any resistance exists in the material, a voltage will appear across the other two points in accordance with Ohm's law (voltage equals current times resistance). When the material enters a superconductive state, its resistance drops to zero and no voltage appears across the second set of points [19].

3.13 Applications of Superconductors

The first large scale commercial application of superconductivity was in magnetic resonance imaging (MRI). This is a non-intrusive medical imaging technique that creates a two-dimensional picture of say tumors and other abnormalities within the body or brain. This requires a person to be placed inside a large and uniform electromagnet with a high magnetic field. Although normal electromagnets can be used for this purpose, because of resistance they would dissipate a great deal of heat and have large power requirements. Superconducting magnets on the other hand have almost no power requirements

apart from operating the cooling. Once electrical current flows in the superconducting wire, the power supply can be switched off because the wires can be formed into a loop and the current will persist indefinitely as long as the temperature is kept below the transition temperature of the superconductor.

Superconductors can also be used to make a device known as a superconducting quantum interference device (SQUID). This is incredibly sensitive to small magnetic fields so that it can detect the magnetic fields from the heart (10^{-10} Tesla) and even the brain (10^{-13} Tesla). For comparison, the Earth's magnetic field is about 10^{-4} Tesla. As a result, SQUID are used in non-intrusive medical diagnostics on the brain. The traditional use of superconductors has been in scientific research where high magnetic field electromagnets are required. The cost of keeping the superconductor cool are much smaller than the cost of operating normal electromagnets, which dissipate heat and have high power requirements. One such application of powerful electromagnets is in high energy physics where beams of protons and other particles are accelerated to almost light speeds and collided with each other so that more fundamental particles are produced. It is expected that this research will answer fundamental questions such as those about the origin of the mass of particles that make up the Universe. Levitating trains have been built that use powerful electromagnets made from superconductors. The superconducting electromagnets are mounted on the train. Normal electromagnets, on a guide way beneath the train, repel (or attract) the superconducting electromagnets to levitate the train while pulling it forwards.

A use of large and powerful superconducting electromagnets is in a possible future energy source known as nuclear fusion. When two light nuclei combine to form a heavier nucleus, the process is called nuclear fusion. This results in the release of large amounts of energy without any harmful waste. Two

isotopes of hydrogen, deuterium and tritium, will fuse to release energy and helium. Deuterium is available in ordinary water and tritium can be made during the nuclear fusion reactions from another abundantly available element – lithium. For this reason it is called clean nuclear energy. For this reaction to occur, the deuterium and tritium gases must be heated to millions of degrees so that they become fully ionized. As a result, they must be confined in space so that they do not escape while being heated. Powerful and large electromagnets made from superconductors are capable of confining these energetic ions. It is expected that this will demonstrate energy production using nuclear fusion [14].

Chapter Four

Practical

4.1 Introduction

The sample under study constitutes a series of four components. They are a part of oxide-compositions, which are created from mixtures of oxides of component elements Ba, Pb, Ca, Cu, by heating in air, at high temperatures (higher than 860 °C).

4.2 Equipment Used in Preparation of the Sample

- Sensitive balance.
- Gate mortar.
- Ceramic boat.
- Furnace.
- Hydraulic press

4.3 The Sample Preparation

. Purity powders of barium carbonate (BaCO_3), lead oxide (PbO_2), calcium oxide (CaO) and cooper oxide (CuO) were used as starting materials.



Figure (4.1) Sensitive balance



Figure (4.2) Furnace



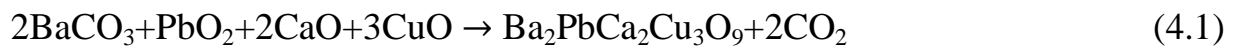
Figure (4.3) Gate mortar



Figure (4.4) Ceramic boat.

4.4 Description Sample Preparation

The calculated weight depends on molecular weights of these Oxides and carbonates with appropriate weights in proportion to their molecular weights through the following chemical reaction



The synthesis of specimens have been performed by solid state reaction method, the powders were mixed together by using a gate mortar with grinding time of about 50 minutes .Then the powders were pressed into disc shape of (25 mm in diameter and 5 mm thickness) using hydraulic press under a pressure of (10 ton/cm²) to insure a uniform transmission of pressure during compact and high density. The specimen were heated using furnace at 860 °C for 24 hours, in order to remove the CO₂ from the mixture as gas and then crushed into fine powder, and then cooled to the room temperature.

4.5 Measuring the Electrical Resistance

4.5.1 Used Equipment

- DC multimeter (Used to read current I).
- DC digital voltmeter (used to read voltage V).
- DC digital voltmeter (used to read voltage V_{23}).
- DC power supply (used for constant voltage supply).
- Thermocouple.
- Connecting wires.
- Ice water bath.

4.5.2 Method Description of Measuring The Electrical Resistance

The experiment involved the use of the four-point probe method, which consists of using separate pairs of current-carrying and voltage-sensing electrodes that are attached to the superconductor. The circuit was constructed for the experiment, as in figure (4.5).

In figure (4.5) the ends of the four-point probe numbered 1,2,3,4, which are connected to the superconductor. Probes 1 and 4 are the current-carrying probes. Probes 2 and 3 are the voltage-sensing probes. Also in this figure, notice that a constant voltage source was used. Due to this setup, a resistance was needed to create a constant current. V_{23} represents the voltage difference between the two terminal points on the superconductor. Use a thermocouple connected to a dc voltmeter (V). A thermocouple is made from two different metal wires (typically copper and constantan) that naturally produce a small voltage difference when subjected to a temperature difference. The outermost ends of the wires will be connected to the sample, while the other ends are immersed in ice. The voltage difference is measured and compared to a standard table of

experimentally determined values. Use this table for converting thermocouple voltage readings to temperature (in K).

To begin the experiment a voltage source was applied across the resistor in order to induce a constant current across the superconductor (current I was kept constant at 100 mA). The sample resistance (R) is calculated by Ohm's Law ($R = V_{23} / I$).

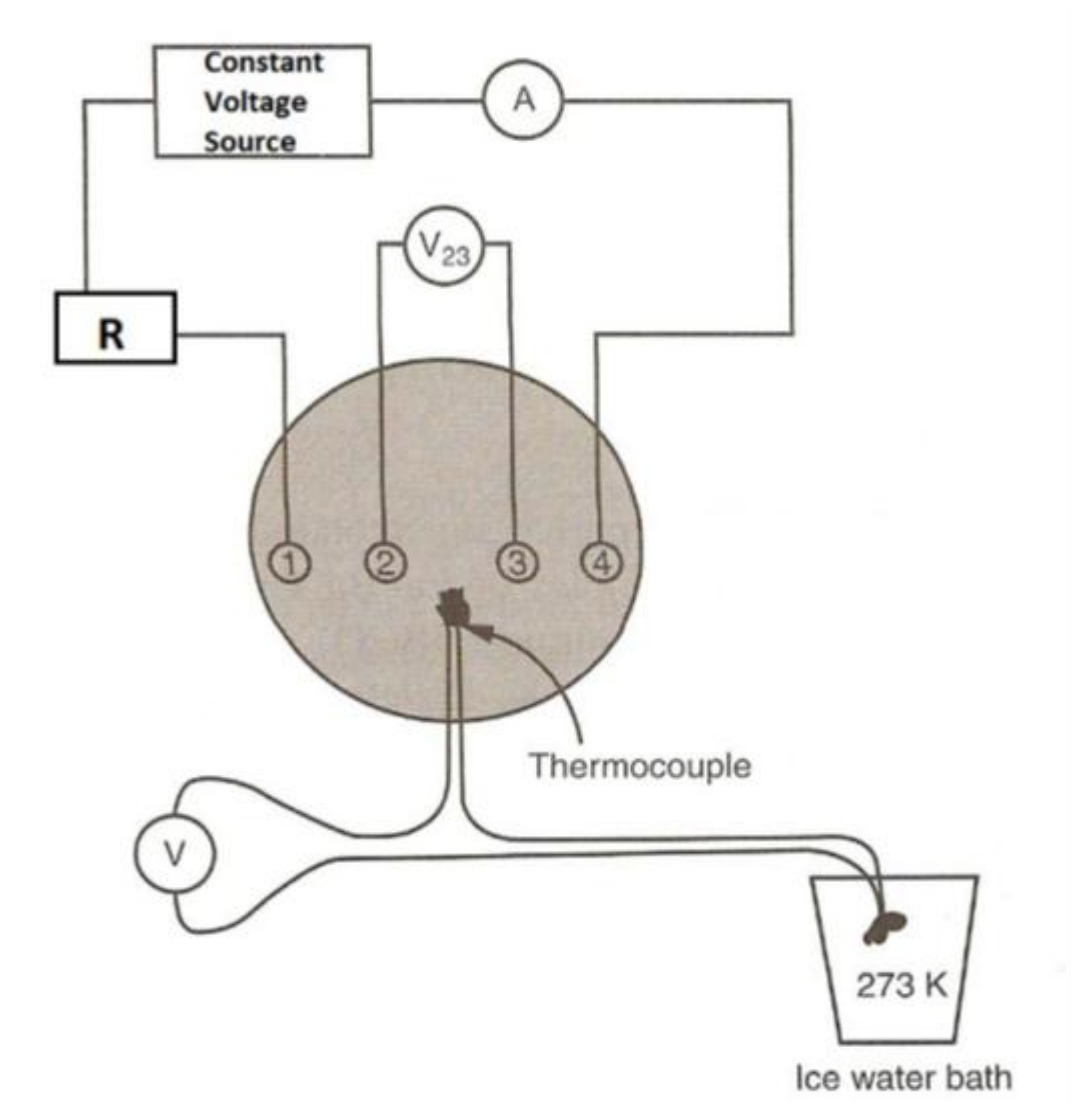


Figure (4.5) Circuit diagram

4.6 Results

For $I = 100 \text{ mA}$

| $V_{23}(\text{mV})$ ± 0.001 | $R(\Omega)$ ± 0.001 | $V(\text{mV})$ ± 0.001 |
|--|--|---|
| 7.7 | 0.077 | 1.43 |
| 10.5 | 0.105 | 1.45 |
| 11.9 | 0.119 | 1.41 |
| 12.7 | 0.127 | 1.44 |
| 13.3 | 0.133 | 1.44 |
| 13.7 | 0.137 | 1.44 |
| 14.4 | 0.144 | 1.47 |
| 14.5 | 0.145 | 1.47 |
| 14.9 | 0.149 | 1.43 |
| 14.1 | 0.144 | 1.42 |
| 15.4 | 0.154 | 1.42 |
| 15.7 | 0.157 | 1.45 |
| 15.8 | 0.158 | 1.45 |
| 15.9 | 0.159 | 1.46 |
| 16.1 | 0.161 | 1.47 |
| 16.3 | 0.163 | 1.48 |
| 16.6 | 0.166 | 1.47 |
| 16.9 | 0.169 | 1.44 |

| V₂₃(mV) ±0.001 | R(Ω) ±0.001 | V(mV) ±0.001 |
|--|------------------------------|--------------------------------|
| 17.1 | 0.171 | 1.43 |
| 17.5 | 0.175 | 1.45 |
| 17.7 | 0.177 | 1.47 |
| 17.9 | 0.179 | 1.45 |
| 18.1 | 0.181 | 1.43 |
| 18.2 | 0.182 | 1.42 |
| 00.0 | 0.000 | 1.45 |
| 00.0 | 0.000 | 1.43 |
| 00.0 | 0.000 | 1.41 |
| 00.0 | 0.000 | 1.41 |
| 00.0 | 0.000 | 1.43 |
| 00.0 | 0.000 | 1.43 |
| 00.0 | 0.000 | 1.43 |
| 00.0 | 0.000 | 1.42 |
| 00.0 | 0.000 | 1.42 |

4.7 Discussion

From the results of this experiment, it was observed appears voltage through the sample and dropped to zero. The appearance of voltage indicates the presence of resistance in the sample and the disappearance of voltage mean the resistance drops to zero. Converting thermocouple voltage readings (V) to temperature, the sample enters a superconductive state at a temperature near 298K.

4.8 Conclusion

In this research the superconductivity near 298K was observed in the $\text{Ba}_2\text{PbCa}_2\text{Cu}_3\text{O}_9$ superconductor.

4.9 Recommendation

- To prepare superconductor that require providing using highly pure materials and special labs to procedure interactions that take place at high temperatures.
- Study the effect of offsetting other oxides, such as the zinc oxide (ZnO) rather than lead oxide, on the critical temperature of the component $\text{Ba}_2\text{PbCa}_2\text{Cu}_3\text{O}_9$.

References

- [1] Christopher Albert, Max Sorantin, Benjamin Stickler,(2011), Advanced Solid State Physics,TU Graz, SS.
- [2] Rao, C. N. R. and A. K. Raychaudhuri, (1996, High Temperature Superconductors, CRC Handbook of Chemistry and Physics. 77th ed. Lide, David R. ed. Boca Raton: CRC Press, 12-84).
- [3] Yoshino, H., Z Bayindir, J. Roy, B. Shaw, H. Ha, A. Lebed, and M. J. Naughton, (2006), “Unconventional Field Dependence of Magneto resistance of $(\text{TMTSF})_2\text{ClO}_4$ Studied by a 46-T Pulsed Magnetic Field System.” Journal of Low Temperature Physics 142.3/4: 319-322).
- [4] M. Tinkham,(1996), Introduction to superconductivity, 2nd ed., McGraw-Hill.
- [5] James F. Annett, (2003), Superconductivity, University of Bristol.
- [6] Andrei Mourachkine, (2003), Room-Temperature Superconductivity, University of Cambridge, Cambridge, United Kingdom.
- [7] M. Lagues, (2005), Proceedings of the NATO Advanced Research Workshop on New Trends in Superconductivity, Yalta, Ukraine, edited by S. Kruchinin and J.
- [8] R. Baquero,(2001), Brief Introduction to Superconductivity, University of Cinvestav. Annett, Kluwer, Dordrecht.
- [9] Widad M. Faisal1 and Salwan K. J. Al-Ani , (1994) , Anlage , S.M. , Wu , D. - H. , Mao , J. , Mao ,S.N. , Xi , X.X. , Venkatesan , T. , Peng , J.L. ,and Greene , R.L., Phys. Rev. , B 50 ,523.
- [10] G. Burns, (1992), High-Temperature Superconductivity, Academic Press, New York.
- [11]Maeda, H., Tanaka, Y., Fukutomi, M., and Asano, (1988), Superconductivity , Jpn. J. Appl. Phys., 27, L209.

- [12] A. Schilling, (1993), Enhanced superconducting properties of the Pb doped trilayer high-temperature, *Nature* 363, 56.
- [13] K.A.Lokshin, (2012), Microstructure and properties of High superconductors, XX 1, 7779P, ISBN: 978-3-642-344.
- [14] E.V. Antipov, (2014). P. Rani et al, *Physic C* 497.
- [15] H.Kleinert, (1982), Disorder Version of the Abelian Higgs Model and the Order of the Superconductive phase Transition, (PDF). *Letter al Nuovo Cimento* 35 (16):405-412. Doi: 10.1007/BF02754760.
- [16] Lev D.Landau;Evgeny M. Lifschitz, (1984), *Electrodynamics of continuous Media. Course of Theoretical Physics 8.* Oxford: Butterworth-Heinemann, ISBN 0-7506-2634-8.
- [17] H. K. Onnes, (1911), the resistance of pure mercury at helium temperatures, *Commun.phys.Lab. Leiden* 12:120.
- [18] R.L.Dolecek, (1954), Adiabatic Magnetization of a Superconducting Sphere, *Physical Review* 96 9(1): 25-28.Bibcode: 1954PhRv...96...25D.doi: 10.1103/PhysRev.96.25.
- [19] J. G. Bednorz and K. A. Müller, (1986), possible high T_C superconductivity in Ba-La-Cu-O system, *Z. Physic B* 64 (1): 189-193. Bibcode: 1986ZPhyB...64...189B. doi: 10.1007/BF01303701.